Inorg. Chem. **2004**, *43*, 3090–3097

Synthesis, Structure, and Dynamics of Nickelacarboranes Incorporating the [*nido*-7,9-$C_2B_9H_{11}$]$^{2-}$ Ligand

Bruce E. Hodson, Thomas D. McGrath, and F. Gordon A. Stone*

Department of Chemistry & Biochemistry, Baylor University, Waco, Texas 76798-7348

Received December 18, 2003

The nickelacarboranes [NEt_4][2-(η^3-C_3H_4R)-*closo*-2,1,7-$NiC_2B_9H_{11}$] (R = H (**1a**), Ph (**1b**)) have been synthesized via reaction between [Na]$_2$[*nido*-7,9-$C_2B_9H_{11}$] and [$Ni_2(\mu$-Br$)_2(\eta^3$-$C_3H_4R)_2$] in THF (THF = tetrahydrofuran), followed by addition of [NEt_4]Cl. Protonation of **1a** in the presence of a donor ligand L affords the complexes [2,2-L_2-*closo*-2,1,7-$NiC_2B_9H_{11}$] (L = CO (**2**), $CNBu^t$ (**3**)). Addition of PEt_3 (1 equiv) to **2** produces quantitative conversion to [2-CO-2-PEt_3-*closo*-2,1,7-$NiC_2B_9H_{11}$], **4**. Species **2**–**4** exhibit in solution hindered rotation of the NiL_2 fragment with respect to the η^5-C_2B_9 cage unit. Protonation of **1a** in the presence of a diene affords the neutral complexes [2-(η^2:η^2-diene)-*closo*-2,1,7-$NiC_2B_9H_{11}$] (diene = C_5Me_5H (**5**), dcp (**6**), cod (**7**), nbd (**8**), chd (**9**), and cot (**10a**); dcp = dicyclopentadiene, cod = 1,5-cyclooctadiene, nbd = norbornadiene, chd = 1,3-cyclohexadiene, and cot = cyclooctatetraene). Variable temperature ^{1}H NMR experiments show that the {Ni(diene)} fragments are freely rotating even at 193 K. A small quantity of the di-cage species [2,2′-μ-(1,2:5,6-η-3,4:7,8-η-cot)-(*closo*-2,1,7-$NiC_2B_9H_{11})_2$] (**10b**) is formed as a coproduct in the synthesis of **10a**. This species can be rationally synthesized by protonation of **1a** and subsequent addition of **10a**.

Introduction

Since the discovery of the isolobal relationship between the cyclopentadienide anion [C_5H_5]$^-$ and the open face of the dicarbollide ligand [*nido*-7,8-$C_2B_9H_{11}$]$^{2-}$, many transition metal complexes of the latter have been synthesized.[1] However, metallacarboranes derived from the isomeric [*nido*-7,9-$C_2B_9H_{11}$]$^{2-}$ species are relatively rare, there being only a handful of such compounds reported in the literature.[2] The alternative distribution of the carbon atoms in the ligating face of the 7,9-system provides an interesting comparison to their 7,8-counterparts due to the contrasting arrangement of their frontier molecular orbitals.[3] This distinction gives rise to a different preferential orientation of the metal−ancillary ligand fragment with respect to the ligating carborane in each case. Moreover, an appreciable activation barrier to rotation of the metal fragment with respect to the η-bound ligand exists in the 7,9-system. This phenomenon has been observed in complexes of [*nido*-7,9-$C_2B_9H_{11}$]$^{2-}$ with ruthenium,[4] rhodium,[4] and platinum,[3d] but not hitherto in nickel systems. To our knowledge, fully characterized nickel complexes of the [*nido*-7,9-$C_2B_9H_{11}$]$^{2-}$ carborane are restricted to full sandwich compounds[5] and a bipyridyl-Ni-cage species.[6] Closely related to these are a pair of 7-vertex nickelacaborane clusters, namely [1-(tmeda)-2,4-$(SiMe_3)_2$-*closo*-1,2,4-$NiC_2B_4H_4$] (tmeda = *N*,*N*,*N*′,*N*′-tetramethyleth-

* To whom correspondence should be addressed. E-mail: gordon_stone@baylor.edu.

(1) (a) Saxena, A. K.; Maguire, J. A.; Hosmane, N. S. *Chem. Rev.* **1997**, *97*, 2421. (b) Grimes, R. N. In *Comprehensive Organometallic Chemistry*; Wilkinson, G., Abel, E. W., Stone, F. G. A., Eds.; Pergamon Press: Oxford, U.K., 1982; Vol. 1, Section 5.5. (c) Grimes, R. N. In *Comprehensive Organometallic Chemistry II*; Abel, E. W., Stone, F. G. A., Wilkinson, G., Eds.; Pergamon Press: Oxford, U.K., 1995; Vol. 1 (Housecroft, C. E., Ed.), Chapter 9. (d) Grimes, R. N. *Coord. Chem. Rev.* **2000**, *200*−*202*, 773.

(2) For recent examples see: Batsanov, A. S.; Eva, P. A.; Fox, M. A.; Howard, J. A. K.; Hughes, A. K.; Johnson, A. L.; Martin, A. M.; Wade, K. *J. Chem. Soc., Dalton Trans.* **2000**, 3519. Vinas, C.; Gomez, S.; Bertran, J.; Barron, J.; Teixidor, F.; Dozol, J. F.; Rouquette, H.; Kivekas, R.; Sillanpaa, R. *J. Organomet. Chem.* **1999**, *581*, 188. Gruner, B.; Cisarova, I.; Franken, A.; Plesek, J. *Tetrahedron: Asymmetry* **1998**, *9*, 79. Welch, A. J.; Weller, A. S. *J. Chem. Soc., Dalton Trans.* **1997**, 1205.

(3) (a) Albright, T. A.; Hoffman, R. *Chem. Ber.* **1978**, *111*, 1578. (b) Mingos, D. M. P. *J. Chem. Soc., Dalton Trans.* **1977**, 602. (c) Mingos, D. M. P. *J. Organomet. Chem.* **1979**, *181*, 169. (d) Mingos, D. M. P.; Forsyth, M. I.; Welch, A. J. *J. Chem. Soc., Chem. Commun.* **1977**, 605. (e) Mingos, D. M. P.; Forsyth, M. I.; Welch, A. J. *J. Chem. Soc., Dalton Trans.* **1978**, 1363.

(4) Marder, T. B.; Baker, R. T.; Long, J. A.; Doi, J. A.; Hawthorne, M. F. *J. Am. Chem. Soc.* **1981**, *103*, 2988.

(5) (a) Wing, R. M. *J. Am. Chem. Soc.* **1970**, *92*, 1187. (b) Varadarajan, A.; Johnson, S. E.; Gomez, F. A.; Chakrabarti, S.; Knobler, C. B.; Hawthorne, M. F. *J. Am. Chem. Soc.* **1992**, *114*, 9003.

(6) Erdman, A. A.; Zubreichuk, Z. P.; Prokopovich, V. P.; Polyakov, A. V.; Yanovsky, A. I.; Maier, Yu. N. A.; Ol'dekop, A. *Koord. Khim. (Russ.)* **1989**, *15*, 122.

10.1021/ic035458r CCC: $27.50
Published on Web 04/20/2004

Scheme 1

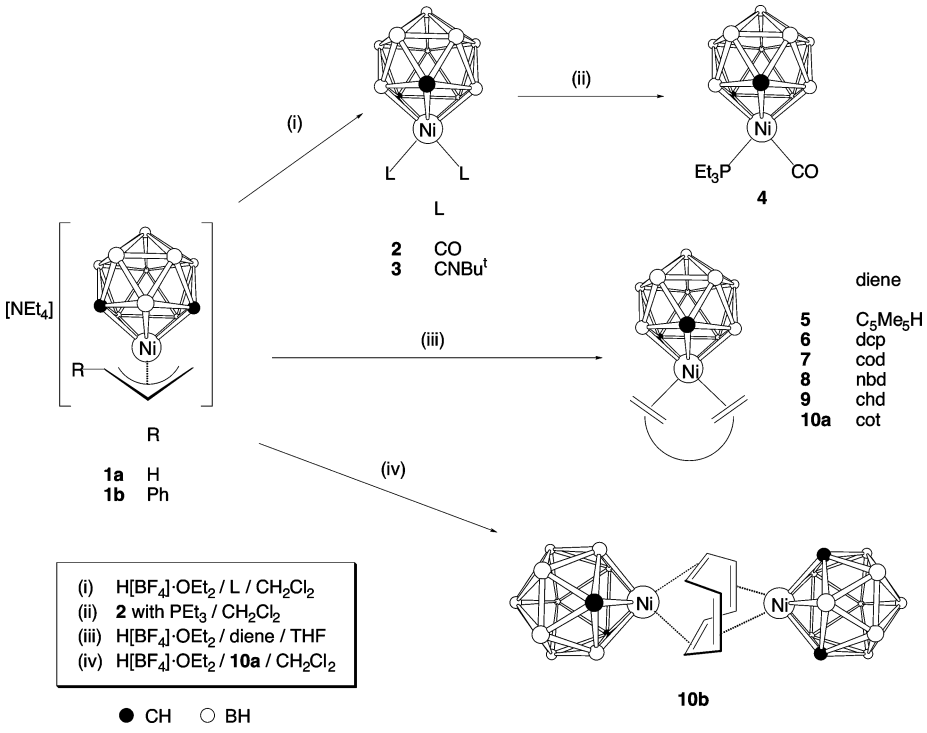

ylenediamine) and [*commo*-1,1′-Ni-{2,4-$(SiMe_3)_2$-*closo*-1,2,4-$NiC_2B_4H_4$}$_2$].[7] These also involve the "carbons apart" arrangement in the nickel-bound five-membered carborane face. More elaborate examples, in which the nickel vertex is bonded to carborane ligands with six-membered open faces, include the 11-vertex tricarborane complexes [1-(η^3-2′-R-C_3H_4)-2-Me-*closo*-1,2,3,5-$NiC_3B_7H_9$] (R = H, Me)[8] and 13-vertex [4-(η^3-C_3H_5)-1,6-Me_2-*closo*-4,1,6-$NiC_2B_{10}H_{10}$].[9] Herein we describe the synthesis and characterization of several nickelacarboranes containing the [*nido*-7,9-$C_2B_9H_{11}$]$^{2-}$ ligand. These compounds provide examples of both hindered and free rotation of the metal ligand fragment with respect to the η^5 ligating face.

Results and Discussion

The nickel complexes [NEt_4][2-(η^3-C_3H_4R)-*closo*-2,1,7-$NiC_2B_9H_{11}$] (R = H (**1a**), Ph (**1b**); Scheme 1) were prepared via reaction of [Na]$_2$[*nido*-7,9-$C_2B_9H_{11}$] (generated in situ from [$NHMe_3$][*nido*-7,9-$C_2B_9H_{12}$] and NaH) with [Ni_2(μ-Br)$_2$(η^3-C_3H_4R)$_2$] at −50 °C in THF, with subsequent addition of [NEt_4]Cl. Compound **1a** is the analogue of [NEt_4]-[3-(η^3-C_3H_5)-1,2-Me_2-*closo*-3,1,2-$NiC_2B_9H_9$],[10] which contains the "carbons adjacent" {*nido*-7,8-C_2B_9} moiety. An $^{11}B\{^1H\}$ NMR study of **1a** shows signals due to the carborane cage in a 2:2:1:1:2:1 intensity ratio, indicating mirror symmetry, and its ^1H NMR spectrum reveals a pair of doublets and an unresolved triplet of triplets due to the allyl group (methylene protons at δ 3.04 and 2.00 and methine proton at δ 5.15, respectively). Carborane CH groups are observed as a broad resonance at δ 1.72 in the latter spectrum. The related compound [NEt_4][2-(η^3-C_3H_4Ph)-*closo*-2,1,7-$NiC_2B_9H_{11}$] (**1b**), prepared similarly, showed signals in its $^{11}B\{^1H\}$ NMR spectrum indicating an asymmetric cage system (1:1:2:1:1:3 intensity ratio); the ^1H NMR spectrum revealed individual multiplets for each of the protons of the allyl group (δ 5.32 (methine CH), 3.58 (C*H*Ph), 3.08 (syn CH_2), 2.17 (anti CH_2)) and a broad singlet for the carborane CH groups (δ 2.19, two coincident resonances).

Diffraction quality crystals of **1a** were obtained, but these fractured on cooling to the low temperatures preferred for X-ray structural analyses. Accordingly, a crystallographic study was carried out upon **1b**, affording the structure shown in Figure 1. In the solid state the allyl moiety is aligned so that the C(11)−C(21) vector lies approximately within the plane defined by B(3)B(9)B(10). Although C(12) and C(13) of the hydrocarbon ligand suffer from partial disorder across the latter plane, only one conformer is evident, namely that in which the phenyl substituted terminus lies over the B(6)−B(11) connectivity. The C_2B_3 ligating face is folded into an envelope configuration, favoring long Ni−C distances (φ = 7.4°, θ = 3.6°) with the nickel atom slipped[3d] by −0.04 Å with respect to the centroid of the lower B_5 pentagonal belt. These distortions are a result of the localization of the core molecular orbitals of the carborane open face on the carbon atoms, and are discussed further below.

Addition of the acid H[BF_4]·OEt_2 to a cooled (−50 °C), CO-saturated solution of **1a** in CH_2Cl_2 releases the allyl group as CH_2=CHMe with formation of neutral [2,2-$(CO)_2$-

(7) Zhang, H.; Wang, Y.; Saxena, A. K.; Oki, A. R.; Maguire, J. A.; Hosmane, N. S. *Organometallics* **1993**, *12*, 3944.
(8) Weinmann, W.; Wolf, A.; Pritzkow, H.; Siebert, W.; Barnum, B. A.; Carroll, P. J.; Sneddon, L. G. *Organometallics* **1995**, *14*, 1911.
(9) Mullica, D. F.; Sappenfield, E. L.; Stone, F. G. A.; Woollam, S. F. *Can. J. Chem.* **1995**, *73*, 909.
(10) Carr, N.; Mullica, D. F.; Sappenfield, E. L.; Stone, F. G. A. *Inorg. Chem.* **1994**, *33*, 1666.

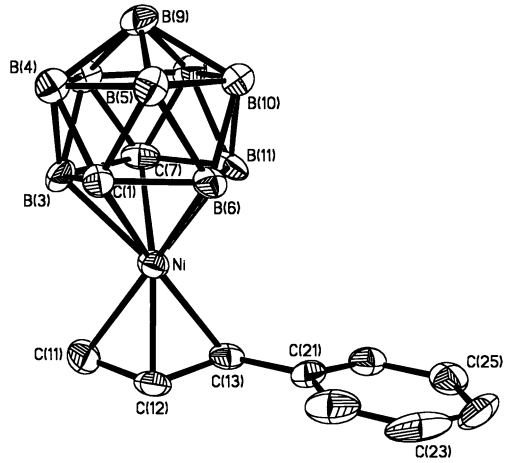

Figure 1. Structure of the anion of compound **1b**, showing the crystallographic numbering scheme. In this and in Figures 3−5, thermal ellipsoids are drawn at the 40% probability level, and H atoms are omitted for clarity. Selected interatomic distances (Å) and angles (deg) are Ni−C(11) 2.030(8), Ni−C(12) 1.943(9), Ni−C(13) 2.032(9), Ni−C(1) 2.147(7), Ni−B(3) 2.082(8), Ni−B(6) 2.096(7), Ni−C(7) 2.146(7), Ni−B(11) 2.096(8), C(11)−C(12) 1.395(14), C(12)−C(13) 1.411(17), C(13)−C(21) 1.485(13); C(12)−Ni−C(11) 41.0(4), C(12)−Ni−C(13) 41.5(5), C(11)−Ni−C(13) 71.7(4), C(11)−C(12)−C(13) 116.0(10), C(12)−C(13)−C(21) 121.9(9), Ni−C(13)−C(21) 122.5(6).

closo-2,1,7-$NiC_2B_9H_{11}$] (**2**) (Scheme 1). In contrast to the previously prepared analogue [1,2-Me_2-3,3-$(CO)_2$-*closo*-3,1,2-$NiC_2B_9H_9$],[10] compound **2** is relatively stable in the solid state. In CH_2Cl_2 solution under an inert atmosphere, it survives for several days; however, on exposure to air or addition of Me_3NO, rapid decomposition occurs. A sample of **2** suitably pure for elemental analysis was unfortunately not obtained. The infrared spectrum displays broad CO absorptions at 2098 and 2130 cm^{-1}, and two distinct resonances were observed for the carbonyl groups in the $^{13}C\{^1H\}$ NMR spectrum (δ 188.1 and 184.4). Despite this inequivalence, the mirror symmetric nature of the cage system is retained with the $^{11}B\{^1H\}$ NMR spectrum of **2** showing 6 resonances in a 1:2:3(2 + 1 coincidence):2:1 intensity ratio.

The origin of the carbonyl group inequivalence is a barrier to rotation of the $\{Ni(CO)_2\}$ fragment with respect to the ligating pentagonal carborane face. The distribution of the carborane frontier molecular orbitals favors a particular conformation (Figure 2) that allows for optimum overlap of the metal-based ($x-z$) hybrid HOMO (highest occupied molecular orbital) with the carborane LUMO (lowest unoccupied molecular orbital) when the nickel fragment lies in the cage mirror plane.[3] As predicted by Mingos,[3b] a considerable barrier to rotation (i.e., deviation from the most favored conformation) is encountered. Thus, the two carbonyl ligands are rendered inequivalent (Figure 2c), as observed spectroscopically.

These findings are also in agreement with similar results obtained for the related 7-vertex system [1-(tmeda)-2,4-$(SiMe_3)_2$-*closo*-1,2,4-$NiC_2B_4H_4$].[7] The latter species' NMR data at ambient temperatures were consistent with hindered rotation of the {Ni(tmeda)} fragment with respect to the carborane face, although it was noted that the bulky $SiMe_3$ units may also contribute to this. In the solid state, it was

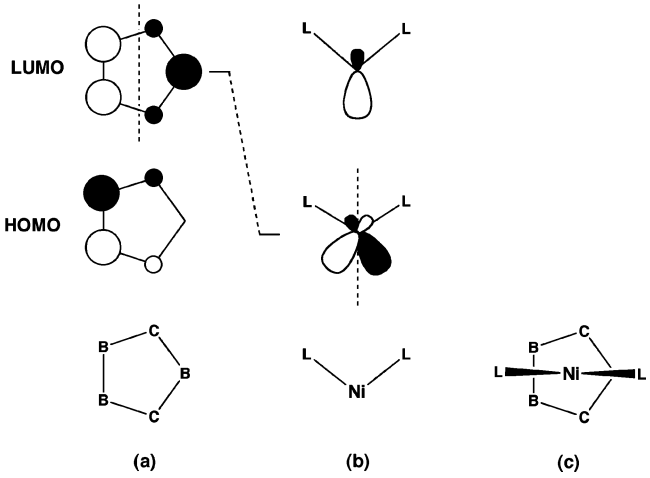

Figure 2. Frontier molecular orbitals of (a) the open face of the {*nido*-7,9-$C_2B_9H_{11}$} unit and (b) the $\{NiL_2\}$ fragment, with (c) their expected relative orientations when HOMO−LUMO interactions are optimized.

likewise found that the nickel fragment was oriented such that the notional $\{NiL_2\}$ plane coincided with the carborane mirror plane. Molecular orbital calculations also predicted this to be the preferred conformation for $\{ML_2\}$ fragments bonded to the face of the "carbons apart" {*nido*-2,4-C_2B_4} ligand; the existence of a barrier to rotation, however, was not evaluated.

In a reaction analogous to the formation of **2**, addition of $H[BF_4]\cdot OEt_2$ to a CH_2Cl_2 solution of **1a** at −50 °C followed by 2 equiv of $CNBu^t$ produced the compound [2,2-$(CNBu^t)_2$-*closo*-2,1,7-$NiC_2B_9H_{11}$] (**3**). The infrared spectrum of **3** shows strong CN absorptions at 2197 and 2178 cm^{-1}. The ^1H NMR spectrum shows resonances due to the cage CH groups (a broad singlet at δ 2.57) and the methyl groups of the isocyanide ligands (a broad singlet at δ 1.45) in a 2:18 intensity ratio. In the $^{13}C\{^1H\}$ NMR spectrum of **3**, two sets of peaks for the isocyanide units are observed. As in **2**, the $^{11}B\{^1H\}$ NMR spectrum indicates that the carborane cage retains C_s symmetry, implying that the metal-bound ligands are lying within the mirror plane of the cage. Again, the presence of unique environments for the isocyanide ligands in this system is ascribed to a barrier to rotation of the $\{Ni(CNBu^t)_2\}$ fragment.

Addition of PEt_3 (1 equiv) to **2** results in substitution of one carbonyl ligand to give [2-CO-2-PEt_3-*closo*-2,1,7-$NiC_2B_9H_{11}$] (**4**). The carbonyl group shows one IR active stretch (possibly two coincidental bands) at 2058 cm^{-1}, significantly to lower energy than those of **2** due to the greater electron density at the nickel atom. As a result of the differing exo-cage ligands, the lack of rotation within the system is more pronounced in the NMR spectra of **4**. Doublet resonances in the $^{13}C\{^1H\}$ NMR spectrum are observed at δ 192.6 (J(PC) = 27 Hz) and 188.7 (J(PC) = 27 Hz) for the single carbonyl group in each of the two possible orientations with respect to the carborane cage. The different orientations of the PEt_3 ligands are evident in the $^{31}P\{^1H\}$ NMR spectrum with two singlet resonances at δ 35.9 and 23.6, and in the ^1H NMR spectrum with two multiplet resonances for both the methylene (δ 1.94 and 1.86) and methyl (δ 1.16 and 1.09) portions of the ethyl groups.

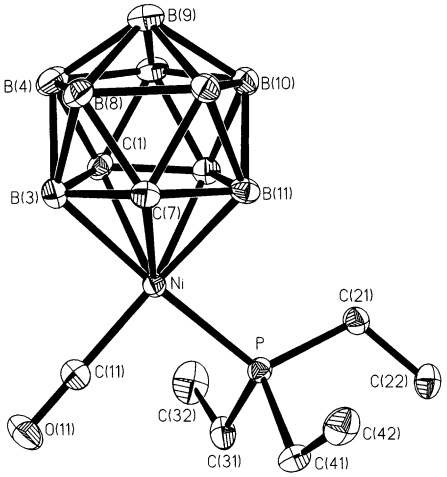

Figure 3. Structure of compound **4**, showing the crystallographic numbering scheme. Selected interatomic distances (Å) and angles (deg) are Ni−C(1) 2.172(4), Ni−B(3) 2.084(5), Ni−B(6) 2.102(5), Ni−C(7) 2.182(4), Ni−B(11) 2.100(5), Ni−P 2.1843(11), Ni−C(11) 1.777(4), C(11)−O(11) 1.134(5); Ni−C(11)−O(11) 179.3(4), C(11)−Ni−P 92.04(14).

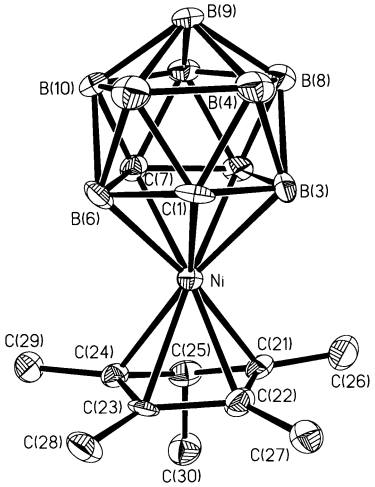

Figure 4. Structure of compound **5**, showing the crystallographic numbering scheme. Selected interatomic distances (Å) and angles (deg) are Ni−C(1) 2.183(6), Ni−B(3) 2.083(8), Ni−B(6) 1.976(8), Ni−C(7) 2.089(6), Ni−B(11) 2.090(8), Ni−C(21) 2.024(6), Ni−C(22) 1.985(6), Ni−C(23) 2.049(6), Ni−C(24) 2.149(7), Ni···C(25) 2.517(6), C(21)−C(22) 1.442(9), C(21)−C(25) 1.529(9), C(22)−C(23) 1.417(9), C(23)−C(24) 1.455(9), C(24)−C(25) 1.480(9); C(22)−C(21)−C(25) 111.8(6), C(23)−C(22)−C(21) 105.6(6), C(22)−C(23)−C(24) 108.1(6), C(23)−C(24)−C(25) 111.2(5), C(24)−C(25)−C(21) 97.1(5), C(25)−C(21)−Ni 89.1(4), C(25)−C(24)−Ni 85.7(4).

An X-ray crystallographic study of **4** revealed the structure shown in Figure 3. There is only one conformation in the solid state, namely that having the phosphine ligand trans to B(3) of the carborane cage. According to trans effect considerations, this is expected to be the more stable arrangement. The nickel atom is slipped away from B(3) by −0.05 Å, and the C_2B_3 ligating face itself is distorted (φ = 7.9 °, θ = 3.8 °). The folding values are larger in the related compound [1,7-Me_2-2,2-$(PMe_2Ph)_2$-*closo*-2,1,7-$PtC_2B_9H_9$][3d] (φ = 11°, θ = 5°), which may be due to the greater electron donating properties of the cage carbon methyl substituents, though the back-bonding capabilities of the carbonyl group in **4** may contribute. Attempts to substitute the carbonyl ligand by isocyanides or alkynes, or to force a dimerization by removal of CO, were unsuccessful.

A complementary series of reactions involving protonation of **1a** in the presence of dienes afforded compounds of formulation [2-(η^2:η^2-diene)-*closo*-2,1,7-$NiC_2B_9H_{11}$] (diene = C_5Me_5H (pentamethylcyclopentadiene) **5**, dcp (dicyclopentadiene) **6**, cod (1,5-cyclooctadiene) **7**, nbd (norbornadiene) **8**, and chd (1,3-cyclohexadiene) **9** (Scheme 1)). The products, formally Ni(II) diene complexes, were readily separated from the reaction mixture by column chromatography and were characterized by the data in Tables 1−3.

The $^{11}B\{^1H\}$ NMR spectrum of **5** showed a pattern of peaks of relative intensity 1:2:2:1:1:2 indicative of the presence of a mirror symmetric cage unit. Three resonances at δ 2.18, 1.70, and 0.87 were observed in the ^1H NMR spectrum due to the Me groups of the C_5Me_5H ring. That at δ 0.87 was a doublet (J(HH) = 7 Hz) and may be assigned to the C(*Me*)H group. Correspondingly, the resonance for the C(Me)*H* proton at δ 3.23 was a quartet (Table 2). The room temperature $^{13}C\{^1H\}$ NMR spectrum showed only three methyl environments (δ 21.9, 11.6, and 11.3). In contrast, a low temperature (193 K) ^1H NMR spectrum revealed separate resonances for each of the five methyl groups (δ 2.21, 2.12, 1.76, 1.61, and 0.85 (doublet)). At room temperature the protons of the carborane cage carbon atoms were visible in the ^1H NMR spectrum as a broad singlet resonance at δ 2.35. At low temperature this became two separate resonances at δ 2.83 and 1.90. These findings are consistent with a static structure at the lower temperature, akin to that determined by X-ray diffraction (see later), and with free rotation of the {Ni(C_5Me_5H)} moiety with respect to the carborane moiety at ambient temperatures. A lower barrier to rotation in comparison to compounds **2**−**4** is presumably due to the more delocalized nature of the bonding in **5** and the differing donor properties of the diene.

The molecular structure of **5**, as determined by an X-ray diffraction experiment, is shown in Figure 4. It is notable that the η^2 binding sites of the C_5Me_5H moiety lie approximately within the mirror plane of the {NiC_2B_9} unit, a situation comparable to that encountered in complexes **2**−**4**. Again, this arrangement allows optimum overlap between the frontier orbitals of the η^5-7,9-C_2B_9 fragment and the {Ni(C_5Me_5H)} (pseudo-ML_2) group. The axial methyl group of the C(H)Me unit is projected away from the carborane ligand, presumably in order to minimize steric interactions. Several attempts were made to remove the unique proton of the hydrocarbon ligand, to form a $[C_5Me_5]^-$ unit. Although a pronounced darkening of the reaction mixture was observed upon addition of Bu^nLi solution to **5** in THF, appearing to confirm that reaction was taking place, the species so formed was extremely susceptible to reprotonation. It is, of course, possible that the site of base attack is an acidic carborane CH group.

The nonconjugated diene dcp was used similarly to prepare [2-(2,3:6,7-η-dcp)-*closo*-2,1,7-$NiC_2B_9H_{11}$] (**6**). The {Ni(dcp)} unit is devoid of symmetry; hence, the $^{11}B\{^1H\}$ NMR spectrum shows a 2:1:1:1:1:1:2 peak intensity ratio. Individual resonances are observed for the cage carbon protons

Table 1. Analytical and Physical Data[a]

compd	color	yield %	anal.[b] (%) C	anal.[b] (%) H
[NEt_4][2-(η^3-C_3H_5)-*closo*-2,1,7-$NiC_2B_9H_{11}$] (**1a**)	red	77	41.1 (40.9)	9.8 (9.1)[c]
[NEt_4][2-(η^3-C_3H_4Ph)-*closo*-2,1,7-$NiC_2B_9H_{11}$] (**1b**)	dark red	38	48.2 (48.7)	8.7 (8.6)[c]
[2,2-$(CO)_2$-*closo*-2,1,7-$NiC_2B_9H_{11}$] (**2**[d])	brown	62		
[2,2-$(CNBu^t)_2$-*closo*-2,1,7-$NiC_2B_9H_{11}$] (**3**)	orange	65	40.5 (40.3)	8.2 (8.2)
[2-CO-2-PEt_3-*closo*-2,1,7-$NiC_2B_9H_{11}$] (**4**)	orange	98	32.5 (32.1)	7.9 (7.8)
[2-(η^2:η^2-C_5Me_5H)-*closo*-2,1,7-$NiC_2B_9H_{11}$] (**5**)	orange	52	43.3(44.0)	8.3 (8.3)
[2-(2,3:6,7-η-dcp)-*closo*-2,1,7-$NiC_2B_9H_{11}$] (**6**)	orange	54	44.5 (44.6)	7.1 (7.2)
[2-(1,2:5,6-η-cod)-*closo*-2,1,7-$NiC_2B_9H_{11}$] (**7**)	orange	55	40.3 (40.1)	7.8 (7.8)
[2-(2,3:5,6-η-nbd)-*closo*-2,1,7-$NiC_2B_9H_{11}$] (**8**)	orange	47	38.2 (38.2)	6.9 (6.8)
[2-(1,2:3,4-η-chd)-*closo*-2,1,7-$NiC_2B_9H_{11}$] (**9**)	orange	42	35.5 (35.4)	7.0 (7.0)
[2-(1,2:5,6-η-cot)-*closo*-2,1,7-$NiC_2B_9H_{11}$] (**10a**)	orange	28	40.7 (40.8)	6.5 (6.5)
[2,2′-μ-(1,2:5,6-η-3,4:7,8-η-cot)-(*closo*-2,1,7-$NiC_2B_9H_{11})_2$] (**10b**)	dark red	23	27.8 (27.3)	5.8 (5.7)

[a] The infrared spectra (CH_2Cl_2) of all compounds show broad, medium-intensity bands at ca. 2550 cm^{-1} due to B−H absorptions; in addition for **2**, ν_{max}(CO)/cm^{-1} 2098 s, 2130 s; for **3**, ν_{max}(N≡C)/cm^{-1} 2197 s, 2178 s; for **4**, ν_{max}(CO)/cm^{-1} 2058 s. [b] Calculated values are given in parentheses; in addition for **1a**, N 3.4 (3.9); for **1b**, N 3.2 (2.9); for **4**, N 7.8 (7.8). [c] Cocrystallizes with 0.5 mol equiv of CH_2Cl_2. [d] A sample of **2** suitably pure for elemental analysis was not obtained (see text).

Table 2. ^1H and ^{13}C NMR Data[a]

compd	$^1H/\delta$ [b]	$^{13}C/\delta$ [c]
1a	5.15 (m, 1H, allylic C*H*), 3.19 (q, *J*(HH) = 7, 8H, NCH_2Me), 3.04 (d, *J*(HH) = 6, 2H, allylic CH_2), 2.00 (d, *J*(HH) = 11, 2H, allylic CH_2), 1.72 (br s, 2H, cage CH), 1.27 (t, 12H, NCH_2*Me*)	95.6 (allylic CH), 52.0 (allylic CH_2), 49.0 (N*C*H_2Me), 41.0 (br, cage C), 7.8 (NCH_2*Me*)
1b	7.45−7.02 (m, 5H, Ph), 5.32 (m, 1H, allylic CH), 3.58 (d, *J*(HH) = 10, 1H, C*H*Ph), 3.15 (br, 8H, NCH_2Me), 3.08 (d, *J*(HH) = 11, 1H, allylic CH_2), 2.19 (br s, 2H, cage CH), 2.17 (d, *J*(HH) = 11, 1H, allylic CH_2), 1.29 (br, 12H, NCH_2*Me*)	128.7, 128.4, 126.6, 124.2 (Ph), 92.4 (allylic CH), 53.2 (allylic *C*HPh), 53.1 (allylic CH_2), 53.0 (N*C*H_2Me), 39.8 (br, cage C), 7.9 (NCH_2*Me*)
2	2.90 (br s, 2H, cage CH)	188.1 (CO), 184.4 (CO), 56.5 (br, cage C)
3	2.57 (br s, 2H, cage CH), 1.45 (br s, 18H, Bu^t)	139.4 (CN), 139.1 (CN), 58.6 (*C*Me_3), 58.3 (*C*Me_3), 49.4 (br, cage C), 30.2 (C*Me*$_3$), 30.1 (C*Me*$_3$)
4[d]	2.65 (br s, 2H, cage CH), 2.36* (br s, 2H, cage CH), 1.94 (dq, *J*(HH) = *J*(PH) = 8, 6H, PCH_2), 1.86* (dq, *J*(HH) = *J*(PH) = 8, 6H, PCH_2), 1.16 (dt, *J*(PH) = 15, 9H, Me), 1.09* (dt, *J*(PH) = 15, 9H, Me)	192.6 (d, *J*(PC) = 27, CO), 188.7* (d, *J*(PC) = 27, CO), 51.9 (br, cage C), 18.5 (d, *J*(PC) = 31, PCH_2), 17.1* (d, *J*(PC) = 28, PCH_2), 8.3 (br, Me), 8.0* (br, Me)
5	3.23 (q, *J*(HH) = 7, 1H, C(*H*)Me), 2.35 (br s, 2H, cage CH), 2.18 (s, 6H, Me) 1.70 (s, 6H, Me), 0.87 (d, 3H, C(H)*Me*); at 193 K: 3.16 (q, *J*(HH) = 7, 1H, C(*H*)Me), 2.83 (br s, 1H, cage CH), 2.21 (s, 3H, Me), 2.12 (s, 3H, Me), 1.90 (br s, 1H, cage CH), 1.76 (s, 3H, Me), 1.61 (s, 3H, Me), 0.85 (d, 3H, C(H)*Me*)	115.7 (*C*(H)Me), 114.9 (Ni*C*(Me)), 110.0 (Ni*C*(Me)), 57.7 (br, cage C), 21.9 (C(H)*Me*), 13.6 (Ni*CMe*), 11.3 (Ni*CMe*)
6	7.99 (s, 1H, =CH), 5.81 (s, 2H, =CH), 5.48 (s, 1H, =CH), 3.54, 3.22, 2.84 (3H), 2.35, 2.12, 1.79 (m × 6, aliphatic CH × 6), 3.48, 3.02, (br s × 2, cage CH)	121.4, 109.8, 107.4, 101.2 (=CH), 61.6, 55.4, 53.1, 46.8, 41.9, 32.9 (aliphatic C × 6), 56.8 (br, cage C × 2)
7	5.61 (br s, 2H, =CH), 5.58 (br s, 2H, =CH), 3.21 (br s, 2H × 2, cage CH), 2.77, 2.68, 2.45, 2.43 (br s × 4, 2H × 4, CH_2 × 4)	111.1, 104.6 (br, =C), 54.5 (br, cage C), 31.0, 29.6 (br, CH_2)
8	5.61 (s, 4H, =CH), 3.87 (s, 2H, CH_2), 3.35 (br s, 2H, cage CH), 1.77 (s, 2H, tertiary CH)	82.0 (br, =CH), 65.5 (CH_2), 54.3 (br, cage C), 47.1 (tertiary CH)
9	6.13 (s, 2H, =CH), 5.51 (s, 2H, =CH), 2.65 (br s, 2H, cage CH), 2.27 (d, *J*(HH) = 14, 2H, CH_2), 1.71 (d, 2H, CH_2); at 193K: 6.30 (s, 1H, =CH), 6.11 (s, 1H, =CH), 5.65 (br s, 2H, =CH), 3.16 (br s, 1H, cage CH), 2.34 (br s, 1H, cage CH), 2.16 (br s, 1H, CH_2), 2.00 (br s, 1H, CH_2), 1.70 (br s, 2H, CH_2)	100.5 (br, =C), 95.7 (br, =C), 54.9 (br, cage C), 22.7 (CH_2)
10a	6.15−5.68 (br m, 8H, cot), 3.66 (br s, 2H, cage CH); at 223 K: 6.17 (m, 4H, =CH), 5.72 (br s, 2H, NiCH), 5.62 (br s, 2H, NiCH), 3.74 (br s, cage CH)	134.3 (br, =CH), 114.7, 107.2 (br, NiCH), 54.7 (br, cage C)
10b	6.22 (br m, 2H, cot), 6.16 (br m, 4H, cot), 6.10 (br m, 2H, cot), 3.81 (br s, 2H, cage CH), 3.72 (br s, 2H, cage CH)	117.5, 114.3, 109.3, 106.0, (cot), 55.6, 54.8 (br, cage C)

[a] Chemical shifts (δ) in ppm, coupling constants (*J*) in hertz; measurements at ambient temperatures, except where indicated, in CD_2Cl_2. [b] Resonances for terminal BH protons occur as broad unresolved signals in the range δ ca. −1 to +3. [c] ^1H-decoupled chemical shifts are positive to high frequency of $SiMe_4$. [d] Occurs as a mixture of two isomers (see text). Where discernible, resonances due to the minor isomer are marked by an asterisk.

(δ 3.48, 3.02) in the ^1H NMR at room temperature, along with a complex set of peaks due to the dcp protons. Variable temperature (193−348 K) ^1H NMR studies did not reveal any resolution of these peaks, thus leaving investigation into any dynamic processes inconclusive. However, it would be reasonable to suggest that in solution free rotation of the {Ni(dcp)} unit occurs at ambient temperatures, as observed in compound **5** and in compounds **7**−**9** below.

Compounds **7**−**9** having the formulation [2-(η^2:η^2-diene)-*closo*-2,1,7-$NiC_2B_9H_{11}$] (diene = cod (**7**), nbd (**8**), chd (**9**)) were prepared in a fashion similar to **5** and **6**. Each compound displayed resonances in its $^{11}B\{^1H\}$ NMR spectrum at room temperature indicating a mirror symmetric cage unit. The ^1H and $^{13}C\{^1H\}$ spectra were also consistent with a symmetric {Ni(diene)} fragment undergoing rapid rotation (Table 2). Low temperature ^1H NMR studies of these

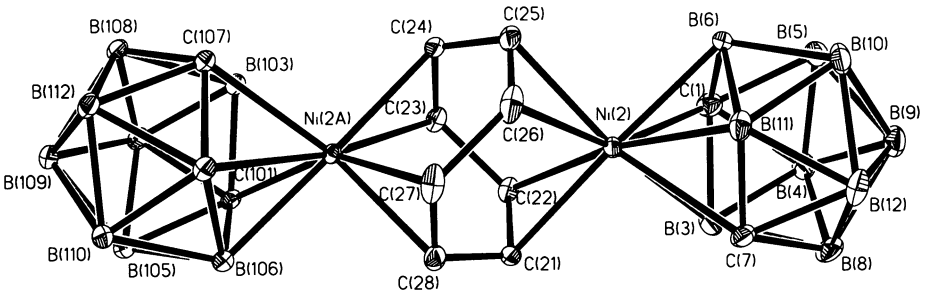

Figure 5. Structure of compound **10b**, showing the crystallographic numbering scheme. Selected interatomic distances (Å) and angles (deg) are Ni(2)−C(1) 2.187(2), Ni(2)−B(3) 2.095(2), Ni(2)−B(11) 2.1207(19), Ni(2)−B(6) 2.1424(19), Ni(2)−C(7) 2.2202(19), Ni(2)−C(22) 2.1314(16), Ni(2)−C(21) 2.1349(17), Ni(2)−C(25) 2.1360(17), Ni(2)−C(26) 2.1632(19), Ni(2A)−C(101) 2.2069(18), Ni(2A)−B(103) 2.0828(19), Ni(2A)−C(107) 2.2040(17), Ni(2A)−B(106) 2.138(2), Ni(2A)−B(111) 2.130(2), Ni(2A)−C(23) 2.1439(18), Ni(2A)−C(24) 2.1626(18), Ni(2A)−C(27) 2.1250(18), Ni(2A)−C(28) 2.1168(18), C(21)−C(22) 1.375(3), C(21)−C(28) 1.483(3), C(22)−C(23) 1.488(2), C(23)−C(24) 1.370(2), C(24)−C(25) 1.481(3), C(25)−C(26) 1.376(3), C(26)−C(27) 1.476(3), C(27)−C(28) 1.386(3); C−C−C range in cot 118.99(16)−120.21(15), Ni−C═C range 70.26(11)−72.41(11), Ni−C−C range 107.31(11)−109.32(12).

compounds failed to arrest the dynamic processes taking place, but revealed some resolution of peak multiplicities in **9**.

The corresponding protonation of the complexes **1** in the presence of cyclooctatetraene yielded a mixture of the mono- and di-cage products [2-(1,2:5,6-η-cot)-*closo*-2,1,7-$NiC_2B_9H_{11}$] (**10a**) and [2,2′-μ-(1,2:5,6-η-3,4:7,8-η-cot)-(*closo*-2,1,7-$NiC_2B_9H_{11})_2$] (**10b**), respectively. Use of 2.5 equiv of the organic ligand gave exclusively **10a**. A room temperature ^{1}H NMR spectrum of **10a** (Table 2) showed a broad singlet peak due to the cage CH protons, and a second very broad multiplet due to those of the cot moiety, which was resolved into an apparent quartet and two singlets (δ 6.17, 5.72 and 5.62, respectively) on cooling to 223 K. Presumably, the high field peaks are due to the protons of the bound ene groups, which retain some unresolved splitting. Hence, the apparent quartet is due to the uncoordinated portion of the cot ligand and results from the coincidence of four overlapping doublets.

A room temperature $^{11}B\{^1H\}$ NMR study of **10b** revealed six broad singlet peaks in a 1:2:2:1:1:2 intensity ratio, indicating essentially equivalent and mirror symmetric carborane cages. However, the ^{1}H NMR study revealed individual resonances for each pair of cage CH groups (δ 3.81 and 3.72, respectively), and in contrast to **10a**, signals due to the cot protons were relatively sharp, appearing as three unresolved multiplets (δ 6.22, 6.16, and 6.10; 2:4:2 ratio). These data suggest that the system is static on the NMR time scale, and that the cages adopt differing orientations with respect to the cot fragment. An X-ray diffraction experiment revealed the molecular structure of **10b**, shown in Figure 5. In the solid state, the Ni-cage moieties are forced to lie essentially orthogonal to one another by the bridging cot unit. As discussed earlier, this orientation allows for optimum HOMO−LUMO interactions between each of the {(η^2:η^2-cot)-Ni} subunits and their respective carborane ligands.

Treatment of **1b** with $H[BF_4]\cdot OEt_2$ followed by addition of **10a** resulted in a 23% conversion to **10b**; however, attempts to coordinate the two remaining "available" alkene moieties in **10a** with other suitable metal fragments, including $[Pt(C_7H_{10})_3]$,[11] $[Co(PPh_3)_2(C_2H_4)_2]$,[12] and $\{Fe(CO)_3\}$,[13] were unsuccessful. Moreover, protonation of **1a** in the presence of $[Rh(\mu\text{-Cl})(1,5\text{-}\eta^2\text{:}\eta^2\text{-}C_8H_8)]_2$[14] in an attempt to attach {Ni(cage)} units to the uncoordinated ene functionalities of the cot ligands failed to produce the desired bimetallic species.

Table 3. ^{11}B NMR Data[a]

compd	$^{11}B/\delta$
1a	−14.5 (2B), −16.9 (2B), −17.6, −23.1, −25.0 (2B), −27.1
1b	−14.1, −14.6, −16.4 (2B), −17.4, −22.7, −24.4 (3B)
2	6.0, −5.2 (2B), −9.8 (3B), −15.3 (2B), −16.9
3	−3.3, −11.1 (2B), −11.5 (2B), −15.8, −19.8 (2B), −22.3
4[b]	−1.1, −8.9, −9.0, −10.9, −11.8, −13.6, −18.1 (2B), −20.6
5	−6.4 (3B), −11.0 (2B), −15.3, −17.9, −19.4 (2B)
6	−1.7 (2B), −7.2, −8.6, −10.3, −13.0, −16.3, −17.8 (2B)
7	−0.9, −6.0 (2B), −9.9 (2B), 12.9, 16.6, 17.2 (2B)
8	−2.1, −6.1 (2B), −10.8 (2B), −13.9 (2B, coincidence), −17.4 (2B)
9	−2.5, −5.9 (2B), −11.3 (2B), −13.1, −16.4, −18.0 (2B)
10a	0.6, −4.9 (2B), −9.8 (2B), −12.1, −13.7, −16.2 (2B)
10b	2.8 (2B), −2.5 (4B), −9.0 (4B), −10.4 (2B), −12.0 (2B), −15.2 (4B)

[a] Chemical shifts (δ) in ppm, measurements at ambient temperatures in CD_2Cl_2. $^{11}B\{^1H\}$ chemical shifts are positive to high frequency of $BF_3\cdot OEt_2$ (external); resonances are of unit integral except where indicated; all resonances display *J*(BH) values of approximately 150 Hz in the ^{11}B spectra. [b] $^{31}P\{^1H\}$ NMR: δ 35.9, 23.6* (* signal due to minor isomer). $^{31}P\{^1H\}$ chemical shifts are positive to high frequency of 85% H_3PO_4 (external).

Addition of other potential "dienes", namely hexamethyl benzene, hexamethyl dewar benzene, indene, cycloheptatriene, and thiophene to the reagents **1** followed by protonation did not yield isolable products. The difficulty of formation of the [2-(C_5Me_5)-*closo*-2,1,7-$NiC_2B_9H_{11}$]$^-$ anion by deprotonation of **5** mentioned above suggests that converting from nonaromatic C_5Me_5H to planar aromatic C_5Me_5 causes instability, possibly due to an excess of electrons about the nickel atom. Conjugation does not seem to be a factor, as both cot and dcp (which contain conjugated and nonconjugated dienes, respectively) formed stable compounds. However, in the case of chd it is remarkable that although the formation of [2-(1,2:3,4-η-chd)-*closo*-2,1,7-$NiC_2B_9H_{11}$] (**9**) was successful, the preparation of an isomer using 1,4-cyclohexadiene was not.

(11) Crascall, L. E.; Spencer, J. L. *Inorg. Synth.* **1990**, *28*, 126.
(12) Nicholls, J. C.; Spencer, J. L. *Inorg. Synth.* **1990**, *28*, 273.
(13) McFarlane, W.; Wilkinson, G. *Inorg. Synth.* **1966**, *8*, 184.
(14) Bennett, M. A.; Saxby, J. D. *Inorg. Chem.* **1968**, *7*, 321.

Conclusions

We have shown that nickelacarboranes incorporating the [*nido*-7,9-$C_2B_9H_{11}$]$^{2-}$ unit are readily available via the reagents **1**. NMR studies on solutions have revealed both static (in the case of compounds **2**−**4**) and dynamic (in the case of **5**−**9** and **10a**) behavior on the NMR time scale at room temperature. The unusual cyclooctatetraene bridged dicage system **10b** has been prepared and fully characterized.

Experimental Section

General Considerations. All reactions were carried out under an atmosphere of dry, oxygen-free nitrogen using Schlenk line techniques. Some subsequent manipulations were performed in the air, where indicated. Solvents were distilled from appropriate drying agents under nitrogen prior to use. Petroleum ether refers to that fraction of boiling point 40−60 °C. Chromatography columns (typically ca. 15 cm in length and ca. 2 cm in diameter) were packed with silica gel (Acros, 60−200 mesh). Filtrations through Celite typically employed a pad 5 cm deep. NMR spectra were recorded at the following frequencies: ^{1}H 360.1, ^{13}C 90.6, ^{31}P 145.8, and ^{11}B 115.5 MHz. The compounds [$NHMe_3$][*nido*-7,9-$C_2B_9H_{12}$][15] and [$Ni_2(\mu\text{-Br})_2(\eta^3\text{-}C_3H_4R)_2$][16] (R = H, Ph) were obtained by literature methods; the reagent [Na]$_2$[*nido*-7,9-$C_2B_9H_{11}$] was prepared in situ and used without isolation. All other reagents were used as received.

Synthesis of [NEt_4][2-(η^3-C_3H_4R)-*closo*-2,1,7-$NiC_2B_9H_{11}$] (R = H, Ph). A filtered solution of [Na]$_2$[*nido*-7,9-$C_2B_9H_{11}$] (generated from [$NHMe_3$][*nido*-7,9-$C_2B_9H_{12}$] (1.15 g, 5.85 mmol) and excess NaH (0.82 g of a 60% dispersion in mineral oil, washed with 3 × 25 mL portions of petroleum ether) at reflux temperature for 12 h in THF) was slowly added to a solution of [$Ni_2(\mu\text{-Br})_2(\eta^3\text{-}C_3H_5)_2$] (1.05 g, 2.93 mmol) in THF held at −50 °C. The mixture was then warmed slowly to 0 °C and stirred for 3 h before addition of [NEt_4]Cl (0.97 g, 5.85 mmol). After warming to room temperature and stirring for 12 h, volatiles were removed in vacuo, and CH_2Cl_2 (30 mL) was added to the residue. Extracts were filtered through a Celite plug. and the filtrate was then concentrated in vacuo to ca. 15 mL before addition of petroleum ether (40 mL), affording a dark red solid which was washed with petroleum ether and dried in vacuo to give [NEt_4][2-(η^3-C_3H_5)-*closo*-2,1,7-$NiC_2B_9H_{11}$] (**1a**) (1.59 g).

Compound **1b** (1.2 g) was prepared in an identical manner, using [$Ni_2(\mu\text{-Br})_2(\eta^3\text{-}C_3H_4Ph)_2$] (3.71 g, 7.27 mmol) as the nickel reagent.

Synthesis of [2,2-$(CO)_2$-*closo*-2,1,7-$NiC_2B_9H_{11}$]. A cooled (−50 °C) CH_2Cl_2 solution (25 mL) of **1a** (0.20 g, 0.56 mmol) was saturated with CO and treated with H[BF_4]·OEt_2 (77 μL, 54% w/w in OEt_2, 0.56 mmol). The mixture was then allowed to warm slowly to 0 °C and stirred at this temperature for 2 h. After this time, the CO source was disconnected, volatiles were removed in vacuo, and the resulting residue was extracted with CH_2Cl_2−petroleum ether (1:4, 2 × 20 mL). The extracts were filtered through a Celite pad and the combined filtrates reduced to dryness in vacuo to yield [2,2-$(CO)_2$-*closo*-2,1,7-$NiC_2B_9H_{11}$] (**2**) (0.09 g) as a light brown powder.

Synthesis of [2,2-$(CNBu^t)_2$-*closo*-2,1,7-$NiC_2B_9H_{11}$]. A cooled (−50 °C) CH_2Cl_2 solution (25 mL) of **1a** (0.12 g, 0.34 mmol) was treated with H[BF_4]·OEt_2 (47 μL, 0.34 mmol) and stirred for 5 min before addition of $CNBu^t$ (77 μL, 0.68 mmol). The mixture was then warmed slowly to room temperature and stirred for 12 h. Volatiles were removed in vacuo, and the resulting residue extracted with CH_2Cl_2−petroleum ether (1:4, 2 × 20 mL). The extracts were filtered through a Celite pad and the combined filtrates reduced to dryness to yield [2,2-$(CNBu^t)_2$-*closo*-2,1,7-$NiC_2B_9H_{11}$] (**3**) (0.08 g) as orange microcrystals.

Synthesis of [2-CO-2-PEt_3-*closo*-2,1,7-$NiC_2B_9H_{11}$]. To a cooled (−50 °C) CH_2Cl_2 solution (25 mL) of **2** (0.09 g, 0.36 mmol) was added PEt_3 (54 μL, 0.38 mmol). The mixture was then warmed slowly to room temperature and stirred for 12 h. Volatiles were removed in vacuo, and the resulting residue was extracted with CH_2Cl_2−petroleum ether (1:4, 2 × 20 mL). The combined extracts were filtered through a Celite pad, and the filtrate was reduced to dryness to yield [2-CO-2-PEt_3-*closo*-2,1,7-$NiC_2B_9H_{11}$] (**4**) as an orange powder, from which orange microcrystals (0.12 g) were grown by solvent diffusion (CH_2Cl_2/petroleum ether).

Synthesis of [2-(η^2:η^2-diene)-*closo*-2,1,7-$NiC_2B_9H_{11}$] Complexes. Pentamethylcyclopentadiene (84 μL, 0.54 mmol) was added to a cooled (0 °C) solution of **1a** (0.19 g, 0.54 mmol) in THF (12 mL). The mixture was stirred for 5 min before addition of H[BF_4]·OEt_2 (74 μL, 0.54 mmol) and subsequent warming to room temperature. After stirring for 1 h, volatiles were removed in vacuo, and the resulting residue was extracted with CH_2Cl_2 (30 mL). The filtered (Celite) extract was reduced in volume to ca. 5 mL in vacuo before being passed down a chromatography column (15 cm in length) using CH_2Cl_2−petroleum ether (1:1) as eluent to yield a single orange band, which was collected and reduced to dryness to yield [2-(1,2:3,4-η-C_5Me_5H)-*closo*-2,1,7-$NiC_2B_9H_{11}$] (**5**) (0.09 g) as a light orange powder.

Compounds **6**−**10a** were prepared using a similar procedure to that described for **5**, replacing pentamethylcyclopentadiene by the appropriate hydrocarbon, namely dicyclopentadiene (**6**), 1,5-cyclooctadiene (**7**), norbornadiene (**8**), 1,3-cyclohexadiene (**9**), or cyclooctatetraene (**10a**).

Synthesis of [2,2′-μ-(1,2:5,6-η-3,4:7,8-η-cot)-(*closo*-2,1,7-$NiC_2B_9H_{11}$)$_2$]. The acid H[BF_4]·OEt_2 (27.9 μL, 0.18 mmol) was added to a cooled (−50 °C) CH_2Cl_2 solution (12 mL) of **1b** (80 mg, 0.18 mmol). The mixture was stirred for 5 min before addition of **10a** (54 mg, 0.18 mmol). After stirring for 1 h, the solution was reduced to approximately 5 mL in vacuo before being passed down a chromatography column using CH_2Cl_2−petroleum ether (1:1) as eluent. A single orange band was collected and the solution reduced to dryness. Further chromatography performed upon the residue with CH_2Cl_2−petroleum ether (1:1) as eluent produced unreacted **10a** and [2,2′-μ-(1,2:5,6-η-3,4:7,8-η-cot)-(*closo*-2,1,7-$NiC_2B_9H_{11}$)$_2$] (**10b**) (20 mg) as a dark red powder.

Structure Determinations. Experimental data for compounds **1b**, **4**, **5**, and **10b** are summarized in Table 4. Diffracted intensities for **1b**, **4**, and **5** were collected on an Enraf-Nonius CAD4 diffractometer using Mo Kα X-radiation (λ = 0.71073 Å). Intensity data were corrected for Lorentz and polarization effects after which a numerical absorption correction based on the measurement of crystal faces was applied. For **10b**, X-ray intensity data were collected on a Bruker X8-APEX CCD area-detector diffractometer using Mo Kα X-radiation. Six sets of narrow data "frames" were collected at different values of θ, for 4 and 2 initial values of ϕ and ω, respectively, using 0.5° increments of ϕ or ω. The data frames were integrated using SAINT.[17] The substantial redundancy in data allowed an empirical absorption correction (SADABS)[17] to be applied, on the basis of multiple measurements of equivalent reflections.

(15) Fox, M. A.; Goeta, A. E.; Hughes, A. K.; Johnson, A. L. *J. Chem. Soc., Dalton Trans.* **2002**, 2132.
(16) Fisher, E. O.; Burger, G. *Z. Naturforsch, B: Chem. Sci.* **1961**, *16*, 77.
(17) *APEX 2*, version 1.0-5; Bruker AXS: Madison, WI, 2003.

Table 4. Crystallographic Data for **1b**, **4**, **5**, and **10b**·CH_2Cl_2

	1b	**4**	**5**	**10b**·CH_2Cl_2
formula	$C_{19}H_{40}B_9NNi$	$C_9H_{26}B_9NiOP$	$C_{12}H_{27}B_9Ni$	$C_{13}H_{32}B_{18}Cl_2Ni_2$
fw	438.52	337.27	327.34	571.29
space group	$P2_1/c$	$P2_12_12_1$	$P2_1/c$	$Pca2_1$
a, Å	10.290(2)	9.836(3)	13.276(4)	13.433(3)
b, Å	13.537(4)	13.1850(16)	9.526(2)	14.690(4)
c, Å	17.289(5)	13.262(3)	13.800(3)	13.076(3)
β, deg	93.70(2)		101.62(2)	
V, Å^3	2403.2(11)	1719.8(6)	1709.5(8)	2580.4(11)
Z	4	4	4	4
ρ_{calcd}, g cm^{-3}	1.212	1.303	1.272	1.471
T, K	173(2)	173(2)	173(2)	110(1)
μ(Mo Kα), mm^{-1}	0.814	1.207	1.119	1.672
reflns measured	5286	3319	2865	32861
indep reflns	4675	3001	2603	12891
R_{int}	0.0908	0.0310	0.0426	0.0458
wR2 (all data), R1[a]	0.2385, 0.0774	0.0789, 0.0395[b]	0.1373, 0.0614	0.0830, 0.0380[b]

[a] Refinement was by full-matrix least-squares on all F^2 data: wR2 = $[\sum\{w(F_o^2 - F_c^2)^2\}/\sum w(F_o^2)^2]^{1/2}$; R1 = $\sum||F_o| - |F_c||/\sum|F_o|$ with $F_o > 4\sigma(F_o)$. [b] Flack parameters: for **4**, 0.01(2); for **10b**, 0.011(8).

All structures were solved by direct methods,[17,18] developed by successive difference Fourier syntheses, and refined by full-matrix least-squares on all F^2 data using SHELXTL versions 5.03 or 6.10.[18] All non-hydrogen atoms were assigned anisotropic displacement parameters. The locations of the cage-carbon atoms were verified by examination of the appropriate internuclear distances and the magnitudes of their isotropic thermal displacement parameters. For **1b**, **4**, and **5**, hydrogen atoms were included in calculated positions and allowed to ride on their parent atoms. These hydrogens were assigned fixed isotropic thermal parameters, $U_{iso}(H) = 1.2 \times U_{iso}$(parent) or $U_{iso}(H) = 1.5 \times U_{iso}(C)$ for methyl groups. For **10b**, the hydrogen atoms of the carboranes were located in difference maps and freely refined, while those of the organic moiety were treated as above. Compound **10b** cocrystallized with one disordered molecule of CH_2Cl_2 per formula unit. The carbon atom of the solvate was located at only one site, but two pairs of chlorine atoms were found. These two parts were assigned refining complementary occupancies, which converged to an approximate ratio of 38:62. All four C−Cl bond distances were restrained to reasonable values (1.76(2) Å); a pair of hydrogen atoms was included in calculated positions for each part. Although **4** is not chiral, it crystallizes in a chiral space group, as does compound **10b**; the value of the Flack parameters (0.01(2) and 0.011(8), respectively) indicates that the correct axial system was chosen to describe each structure.[19]

Acknowledgment. We thank the Robert A. Welch Foundation for support (Grant AA-1201). The Bruker X8 APEX diffractometer was purchased with funds received from the National Science Foundation Major Research Instrumentation Program (Grant CHE-0321214).

Supporting Information Available: Crystallographic data in CIF format. This material is available free of charge via the Internet at http://pubs.acs.org.

IC035458R

(18) *SHELXTL* versions 5.03 and 6.10; Bruker AXS: Madison, WI, 1995 and 2000.

(19) Flack, H. D.; Bernardinelli, G. *J. Appl. Crystallogr.* **2000**, *33*, 1143.